RSC Advances

ROYAL SOCIETY OF CHEMISTRY

www.rsc.org/advances

Exploring bridging effect on first hyperpolarizability

Ria Sinha Roy and Prasanta K. Nandi*

Department of Chemistry, Indian Institute of Engineering Science and Technology, Shibpur, Howrah 711 103, India

Abstract

A number of tetradehydrodinaphtho [10] annulene derivatives with varying charge transferring conduits between two naphthalene rings have been considered for the theoretical study of electronic structure and first hyperpolarizability. The BHHLYP, CAM-B3LYP and M06-2X methods along with the 6-311++G(d,p) basis set are used to calculate first hyperpolarizability by analytical evaluation of electric dipole second derivative. The results obtained by different methods are found to be consistent. The ground state polarity and the first hyperpolarizability of tetradehydrodinaphtho [10] annulene can be strongly enhanced by suitable modification of acetylene linkages. Using different ring structures containing electronegative atom(s) at the bridging position the extent of the longitudinal charge transfer and the magnitude of first hyperpolarizability can be enhanced strongly. The furan ring and the heteroazulene ring has been found to be the most effective bridging moieties to enhance the magnitude of static first hyperpolarizability. The variation of first hyperpolarizability has been explained satisfactorily in terms of the two state calculated spectroscopic properties.

Keywords:
Tetradehydrodinaphtho [10] annulene derivatives, DFT methods, Effect of bridging moiety on NLO property, Two state model

1. Introduction

Non linear optical (NLO) material has recently been one of the major challenging research fields because of its potential application in the field of opto electronics, optical computing, dynamic holography, electro-optical, optical switching, optical logic, fluorescence imaging, optical memory, alkali metal cation sensor, optical power limiting and dynamic image processing[1-7]. A great deal of research has been devoted to design various kinds of potential NLO materials the response of which depends on the applied electromagnetic fields of varying frequency, phase etc. The relation between the architecture of a molecule and its non linear response is an important area of research because by understanding the structure-property correlations the NLO property of a material can easily be tuned by selectively varying the structural motif of the molecule.

The use of organic chromophores as NLO materials have significant advantages over the traditional inorganic solids, $LiNbO_3$, KH_2PO_4, $BaTiO_3$, KTP which exhibit rather poor response property[8]. Organic molecules and polymers are promising NLO candidates because of the ease of their structural modifications which help in the efficient design of new molecular systems having high laser damage thresholds, smaller dielectric constant, refractive indices etc. by means of chemical synthetic efforts in conjunction with the computational modelling. The organic molecular species having highly polarizable electronic structure and low-lying charge-transfer excited states, generally, exhibit large NLO coefficients. Most of the second-order NLO-phores, generally have a π-conjugated framework with asymmetrically substituted electron-donor and electron acceptor groups leading to significant longitudinal charge transfer interaction. The NLO property of such molecular systems can be optimized by suitably modifying the structure by introducing donor and acceptor groups[9-15] of increasing strength, designing different architecture D-π-A (electron donor–π-bridge- electron acceptor), D-D-π-A (introducing electron donating group as a lateral moiety into the π

bridge), D-A-π-A (incorporating additional electron withdrawing moiety into the π bridge as internal acceptor) and also by modifying the π electron system[16], altering bond length parameter[17], modifying charge transfer through space like D-S-A type molecules[18], etc. Doping alkali metal atom in electride system[19-21] largely enhances the magnitude of hyperpolarizability. On incorporating different electron deficient and electron rich bridges into the molecular skeleton the intramolecular charge transfer process and the first hyperpolarizability[22] can be strongly modulated. Elongated π systems and twisted chromophores are found to exhibit higher first hyperpolarizability[23].

In the present work, a number of derivatives of highly delocalized tetradehydrodinaphtho [10] annulene have been considered to find the effect of different bridging conduits on the calculated first hyperpolarizability. The molecule tetrahydrodinaphtho [10] annulene belongs to the sandwich-herringbone type structure exhibiting a π-π stacking interaction[24]. The tetradehydrodinaphtho [10] annulene was successfully synthesized, isolated and characterized by Yoshito Tobe[25] et al. In the present investigation, we intended to study the effect of structural modification of acetylene bridges of tetradihydronaptho [10] annulene by keeping the same electron donor and electron withdrawing groups at the two ends of naphthalene rings. Our primary concern is to find the precise role of different electronic bridges on the calculated non linear optical properties of tetradehydrodinaphtho [10] annulene derivatives. The present study is expected to reveal a new structure property correlation which will be useful to the experimentalists in the synthetic strategy to design efficient NLO-phores.

2. Computational methods

The ground state geometry of the chosen molecules have been fully optimized at the B3LYP level for the 6-31+G (d,p) basis set. The stability of each structure has been checked

by calculating vibrational frequencies of all normal modes at the same level. The calculated frequencies are found to be real which confirm the true minimum in the potential hypersurface. The optimized structures are subsequently used in the calculation of electric response properties. In the presence of external homogeneous electric field of magnitude $\mathbf{F_0}$, the induced electric dipole moment of a molecule can be expressed by the following Taylor series expansion

$$\mu = \mu_0 + \alpha F_0 + \frac{1}{2!}\beta F_0^2 + \frac{1}{3!}\gamma F_0^3 \ldots\ldots\ldots\ldots \quad (1)$$

where $\boldsymbol{\mu_0}$ is the permanent dipole moment and the coefficients α, β, and γ are called polarizability, first hyperpolarizability and second hyperpolarizability of the molecule, respectively. The vector-part of static dipole first hyperpolarizability (β_0) has been calculated by using the following expression,

$$\beta_0 = \sqrt{\beta_x^2 + \beta_y^2 + \beta_z^{\,2}} \quad (2)$$

where β_i,s are the components of β vectors lying along the rectangular Cartesian axes. The x-component β_x is given by

$$\beta_x = \beta_{xxx} + \frac{1}{3}\sum_{j \neq x}(\beta_{xjj} + \beta_{jxj} + \beta_{jjx}) \quad (3)$$

The components of linear polarizabilitity and first hyperpolarizability of the investigated molecules are evaluated analytically as implemented in Gaussian 09 program.[26] The NLO properties are calculated by employing the BHHLYP (50% HF + 50% Becke88 + 50% LSDA exchange and LYP correlation)[27], CAM-B3LYP (long range corrected coulombic-attenuating)[28] and M06-2X[29] functionals for the 6-311++G(d,p) basis set. The BHHLYP and CAM-B3LYP functionals have been used widely for calculation of hyperpolarizabilities. Owing to the lack of experimental and previous theoretical result of hyperpolarizabilities of the investigated molecules, a comparison of the calculated results obtained by the present

DFT methods may be useful to find the correct qualitative trend since the magnitude of the calculated hyperpolarizability is generally found to be sensitive to the choice of the DFT functional employed. Among the chosen DFT methods, the CAM-B3LYP functional has been found[30,31] to be more reliable for (hyper)polarizability calculation since it can reproduce the results obtained with other correlated *ab initio* levels. In our previous theoretical work[32,33] it has been noted that the use of 6-311++G(d,p) basis set can give nearly identical results of hyperpolarizability as obtained with the Dunning's correlation consistent basis set augmented by higher angular momentum diffuse functions. With regard to the size of the investigated molecules the 6-311++G(d,p) basis set has been considered to be appropriate to obtain reliable results of first hyperpolarizability.

In order to rationalize the variation of static first hyperpolarizability (β) among the chosen molecules the following two state expression[34,35] corresponding to the most dominant electronic transition have been invoked.

$$\beta_0 \propto \frac{\Delta\mu_{eg} f_{eg}}{\Delta E_{eg}^3} \qquad (4)$$

The spectroscopic quantities in the above equation are the dipole moment difference ($\Delta\boldsymbol{\mu_{eg}}$), transition energy ($\Delta\mathbf{E_{eg}}$) and the oscillator strength $[\boldsymbol{f_{eg}}\ (= \mathbf{(2m_e/3\hbar^2)}\,\mu_{eg}^2\ .\Delta\mathbf{E_{eg}}]$ associated with the electronic transition from the ground state to the predominant charge transfer excited states. The two-state model has been popularly used to optimize[10b,36,37] the first-hyperpolarizability of donor–acceptor substituted molecular systems. The spectroscopic parameters $\Delta\mu_{eg}$, f_{eg} and ΔE_{eg} are inter-related to each other and are solely controlled by (I) the position and strength of donor and acceptor groups and (II) the nature of the charge transferring bridging moiety.

From the above equation, it seems that the magnitude of first hyperpolarizability should be rather more sensitive to the variation of transition energy compared to the other quantities. The spectroscopic properties of about **20** lowest lying singlet excited states have been calculated by using the time dependent DFT (TDDFT) method consisting of the CAM-B3LYP functional and the 6-311++G(d,p) basis set. The TD-DFT method using the range separated CAM-B3LYP functional can give more accurate results of NLO properties and electronic excitation energies compared to the conventional hybrid functionals.[38,39] In order to check the reliability of the TD-CAM-B3LYP method for calculating the spectroscopic quantities for the present molecular system, the λ_{max} value (402 nm) of molecule **1a** calculated by using the conductor like polarization continuum model (CPCM) of solvent in the framework of TD CAM-B3LYP/6-311++G(d,p) method for the dichloromethane solvent (ϵ = 8.93) is compared with the λ_{max} estimated from the UV-VIS spectroscopic result[25] obtained in the same solvent. The theoretical result of λ_{max} agrees within 3.5% of the experimental result. Thus the present theoretical results of spectroscopic parameters should be considered reliable.

3. Result and discussion

3.1 Optimized geometrical structures

The optimized ground state structures of tetradehydrodinaphtho [10] annulene and its derivatives are shown in **Schemes I – III.** Naphthalene ring substituted with NH_2 / NO_2 groups is denoted as donor naphthalene ring / acceptor naphthalene ring, respectively. Tetradehydrodinaphtho and its derivates having acetylene linker are displayed in **Scheme I**. **Scheme II** consists of two five membered rings fused with cyclobutadiene ring (**2a** and **2b**) / furan ring (**2c** and **2d)** as bridging moieties. The structures in **Scheme III** consist of azulene ring (**3a** and **3b**) and heteroazulene ring (with two nitrogen atoms in the larger ring) (**3c** and **3d**) as bridges. In structure **1a** the two acetylene moieties deviate from the linearity as

indicated by $<C_1C_{20}C_{19} = 4.9^0$ (Table 1). It is interesting to note that when naphthalene rings are substituted with donor and acceptor groups the bent angle increases by about 0.3^0 **(1b)** and 2.8^0 (**1c**) with respect to molecule **1a**. However, when two consecutive middle carbon atoms of one acetylene moiety are bonded to carbon atoms of parallel acetylene unit forming the fused cyclobutadiene ring as in structures **2a** and **2b** (**Scheme II)** the bent angle becomes larger, $<C_1C_{20}C_{19} = 161.4^0$ (**2a**) and $<C_{10}C_{11}C_{12} = 160.3^0$ (**2b**) (Table 1). The corresponding bent angle with fused furan ring increases further, 148.4^0 (**2c)** and 148.5^0 (**2d)**. The dihedral angle between the naphthalene ring and the fused cyclobutadiene ring in molecules **2a** ($\tau_{C9C10C1C20} = 1.9^0$) and **2b** ($\tau_{C9C10C1C20} = 2.8^0$) and the same in molecules **2c** (0.04^0**)** and **2d** (1.9^0) indicates that these molecules are nearly planar. However, with azulene ring as the bridging moiety (molecules **3a** and **3b)** the structures are twisted significantly. As can be seen from Table 1 the two rings of azulene are significantly twisted by 27.9^0 (**3a**) and 24.5^0 (**3b**). Also the larger ring of azulene fused to the donor naphthalene makes a dihedral angle 19^0. However, with heteroazulene ring as a bridging conduit (molecules **3c** and **3d, Scheme III)** the structures become almost planar with naphthalene rings on both sides (Table 1).

Let us now find whether the greater bent angle in molecules **2c** (vs. **2a**) and **2d** (vs. **2b**) will have any effect on the polarity of the bridging moiety. For this purpose, we compare the electron density distribution at the bridging position of molecules **2a** and **2c** (**Scheme II**). The three segments of the bridge possess NBO charges: +0.126 (A), +0.442 (B) and -1.029 (C) for molecule **2a;** -0.676 (A), -0.227 (B) and -0.359 (C) for molecule **2c**. This indicates that the extent of longitudinal electron transfer segment A → segment C in **2a** enhances significantly while it reduces substantially in molecule **2c**. The relatively larger electron population in part A compared to regions B and C of molecule **2c** opposes the longitudinal charge transfer which has been reflected by the smaller ground state dipole moment (**12.3** D) and larger LUMO-HOMO energy gap (**0.064** au) compared to that (**19.2** D and **0.060** au) of

molecule **2a**. Designating the donor substituted naphthalene ring as **E** and acceptor substituted naphthalene ring as **F** it has been noted that charge transfer from ring **E** (+0.230) is much larger with heteroazulene bridge (**3c**) compared to that (+0.054) with the azulene bridge (**3a**). This is fairly consistent with the greater accumulation of negative charge in the naphthalene ring **F** with heteroazulene bridge (-2.116) in contrast to the azulene bridge (-0.622). The greater amount of **E** → **F** charge transfer across the heteroazulene bridge is due to the perfect planarity of the later in contrast to the azulene bridge in which case the two rings are twisted. This has been reflected in the NBO calculated net charge on the larger / smaller ring, -0.297 / -0.372 (heteroazulene) *vs.* -0.594 / -0.105 (azulene) although the net charge density on each of the bridging moiety is almost equal.

As discussed above the nature of charge transfer interaction of the investigated molecules has been significantly modulated due to the difference of electronic structure of the bridging units. The calculated frontier orbital interaction energy can provide an additional insight. Generally, the energy of a HOMO (LUMO) of a conjugated hydrocarbon increase (decrease) when an electron donor (acceptor) attaches to it. For a given bridge the acceptor strength increases by incorporating the cyano substituted thiophene ring which results in the substantial lowering of LUMO-HOMO energy gap (**au**) (1c (0.054) *vs*. 1b (0.072); 2b (0.051) *vs*. 2a (0.060); 2d (0.048) *vs*. 2c (0.064); 3b (0.061) *vs*. 3a (0.076); 3d (0.046) *vs*. 3c (0.061)).

3.2 Static first hyperpolarizability

For the chosen molecules the prominent charge transfer interaction takes place along the x axis which is reflected in the magnitude of ground state dipole moment ($\boldsymbol{\mu_g}$) that is almost identical to the x-component ($\boldsymbol{\mu_x}$). Thus this axial component of polarizability and first hyperpolarizability is taken as the longitudinal component. This is evident from the nearly identical magnitudes of $\boldsymbol{\beta_x}$ and $\boldsymbol{\beta_0}$ (Tables 2 – 4**)**. The calculated results of ground state dipole

moment and first hyperpolarizability obtained by different DFT methods (BHHLYP, CAM-B3LYP and M062X) are compared in Tables 2- 4**.** The ground state dipole moment obtained by different methods differs by a narrow margin. By attaching electron donor and acceptor groups at the terminal sites of naphthalene rings of molecule **1a** the dipole moment can be strongly enhanced (**1a<1c<1b**). The introduction of furan ring at the bridge substantially lowers the μ_g value when compared to the cyclobutadiene ring (**2c<2a** and **2d<2b**). The larger ground state dipole moment of molecules **3a** and **3b** compared to molecules **3c** and **3d,** respectively may be due to the twisted structure of azulene. For the chosen molecules the CAM-B3LYP results of β_0 differs from the M06-2X results by about **0.4 – 6.4** % except for molecule **2b and 1a**. The M06-2X β_0 value of the later compared to CAM-B3LYP value is underestimated by about **11.7**%. At the BHHLYP level β_0 value of molecule **2a** is substantially underestimated in comparison to the CAM-B3LYP and M06-2X results. The results of first hyperpolarizability of the chosen molecules calculated by three DFT methods are compared in Fig 1. It can be seen that although β_0 value of a molecule differs at the three levels the general trend remains same. The three methods identically predict the highest magnitude of first hyperpolarizability for each scheme which varies in the order **1c** (**Scheme I)** < **2d** (**Scheme II)** < **3d** (**Scheme III)**. It should be noted that for molecules **1c** and **2d** the M06-2X calculated β_0 is smaller than the CAM-B3LYP results by about **2** %. On the other hand the BHHLYP and M06-2X calculated β_0 values obtained for molecule **3d** are underestimated significantly (by **10.4** % and **6.4** %) compared to the CAM-B3LYP results. However, the BHHLYP β_0 and M06-2X β_0 of this molecule agree within **4.0** %.

3.3 Structural effect on first hyperpolarizability and TDDFT analysis

It will be interesting to find the effect of change of bridging conduit on the calculated first hyperpolarizability. As it has been discussed in last subsection that for an identically substituted naphthalene rings the modification of electronic structure of the bridge moiety

leads to the significant modulation of the charge distribution and hence the polarity of the ground state structure. However, for the same bridge the presence of cyano substituted fused thiophene ring strongly enhances the magnitude of first hyperpolarizability when compared with molecules without the thiophene moiety. In molecules **2a** and **2b** the cyclobutadiene ring and for molecules **2c** and **2d** furan ring imparts rigidity to the bridging moiety. However, the larger ground state dipole moment of molecules **2a** and **2b** results in significant lowering of β_0 value compared to molecules **1b** and **1c**, respectively. The β_0 of molecule **2a** enhances by about **14.2**% (CAM-B3LYP) when a thiophene ring bearing a **–CN** group is fused with the acceptor naphthalene ring (molecule **2b**). On the other hand the incorporation of furan ring in the bridge (molecules **2c** and **2d**) substantially lowers the ground state dipole moment but enhances β_0 by about an order of magnitude when compared to molecules **2a** and **2b**.

We next consider the effect of azulene bridge (molecules **3a** and **3b**) on the NLO property. Owing to the loss of planarity of the azulene ring the longitudinal charge transfer is strongly hindered which results in substantial lowering of first hyperpolarizability. It would be worthwhile to compare the structural changes of the bridging unit on the first hyperpolarizability of molecules **1c**, **2b** and **3b**. On going from **1c** to **2b** the bent angle increases which probably causes a significant lowering of β_0 value of **2b.** However, the loss of planarity of the bridge in molecule **3b** dramatically reduces the magnitude of β_0. On the other hand when hertero-azulene ring has been used as a bridge (molecules **3c** and **3d**) the perfect planarity is maintained between the naphthalene rings. As a result the extent of charge transfer is markedly enhanced leading to rather strong enhancement of β_0 by about 3.4 times (**3c** *vs*. **3a**) and 4.2 times (**3d** *vs*. **3b**). The exceptionally large increase of quadratic polarizability of molecules **3c** and **3d** also arises from the significant charge transfer from the larger ring to the smaller ring. The most effective role of π bridge on the second order NLO property can be found for molecules **1b**, **2c** and **3c** which have planar structures but the ring

structures of the bridge of molecules **2c** and **3c** play a more crucial role in the modulation of longitudinal charge transfer. The NBO calculated results of charge on the acetylene bridge (-0.085), the three rings of molecule **2c** (-0.676 (A), -0.227 (B) and -0.359 (C)) and that of molecule 3**c** (-0.297 and -0.372 on the larger and smaller rings of heteroazulene, respectively) indicates that the excess negative charge density on ring A of molecule **2c** will favour energetically the linear transition in comparison to molecules **1b** and **3c**. This has been reflected in the larger first hyperpolarizability of molecule **2c**. The variation of β_0 is fairly consistent with the bridge atomic charge sum (BACS)[40] of the molecules.

The TD-CAMB3LYP calculated results of spectroscopic properties along with the two state (**eq 4**) calculated values of first hyperpolarizability obtained for the investigated molecules are presented in Table 5. The two-state model has been invoked to explain the variation of first hyperpolarizability (β_0) of the chosen molecules. According to this model the magnitude of first hyperpolarizability is directly proportional to the dipole moment ($\Delta\mu_{eg}$) difference between the excited and ground state, and the oscillator strength (f_{eg}) but inversely proportional to the third power of transition energy (ΔE_{eg}) associated with the crucial electronic transition. The frontier orbital plots are shown in Fig.2. For molecules of **Scheme I** the increase of β_0 in the order **1a<1b<1c** is fairly consistent with the gradual lowering of transition energy and increase of transition moment. The HOMO is mostly concentrated on donor naphthalene ring and LUMO is concentrated on acceptor ring which accounts for the larger transition moment of molecules **1b** and **1c**. The large decrease of first hyperpolarizability of molecule **2a** compared to that of **1b** arises primarily from the significantly smaller dipole moment difference (**0.785** au) of the former compared to that (**3.586** au) of the later. The substantially smaller $\Delta\mu_{eg}$ value of molecule **2a** is explained by the fact that the partly delocalised π electrons in the cyclobutadiene ring do not take part in the longitudinal charge transfer which has been reflected in the HOMO-LUMO pictures of

2a. The rather smaller β_0 (by an order of magnitude) of **2b** compared to its valence isomer **1c** has been attributed to the smaller transition moment (oscillator strength) and dipole moment difference of **2b**. The presence of furan ring (molecule **2c, Scheme II**) increases the dipole moment difference term ($\Delta\mu_{eg}$) rather appreciably when compared to molecule **2a.** This spectroscopic quantity alone can account for the significant enhancement of first hyperpolarizability of molecule **2c**. The distribution of orbital lobes of HOMO and LUMO of molecule **2c** clearly indicates that significant amount of electron transfer occurs upon electronic excitation from regions A and B to C of the molecule (**Scheme II**). When the acceptor side of molecule **2c** is further modified by attaching a cyano substituted thiophene ring (molecule **2d**), the β_0 value increases by almost 47.9% (CAM-B3LYP level). The rather strong enhancement of quadratic polarizability of molecule **2d** compared to **2c** originates from the substantial lowering of ΔE_{eg} value of the former. This is fairly consistent with the two-level calculated results of β_0.

Let us now discuss the effect of azulene bridge on the magnitude of first hyperpolarizability. The loss of planarity between the two rings of azulene and also between the larger ring of azulene and the donor naphthalene ring strongly hinders the extent of longitudinal charge transfer in molecules **3a** and **3b** which results in substantially higher ΔE_{eg} and smaller $\Delta\mu_{eg}$ values in comparison to molecules **3c** and **3d** having planar structures. The higher β_0 of **1c** compared to that of molecules **2b** and **3b** can be attributed to the higher $\Delta\mu_{eg}$ and f_{eg} values of the former. However, the higher β_0 of **2b** than **3b** arises mainly from the substantial lowering of ΔE_{eg} value of **2b**. The significant lowering of ΔE_{eg} of molecule **2c** compared to **1b** and **3c** leads to strong enhancement of β_0 of the former. The relative variation of above spectroscopic parameters reasonably accounts for the strong enhancement of β_0 (by an order) of molecules **3c** (*versus* **3a**) and **3d** (*versus* **3b**)**.** The substantially larger $\Delta\mu_{eg}$ value of molecule **3c** compared to **3a** arises from the enhanced longitudinal charge transfer in the

former which has been reflected in the HOMO-LUMO pictures (Fig.2). The decrease of charge transfer interaction in molecule **3a** is also consistent with the frontier orbital pictures exhibiting a greater accumulation of charge density on the azulene because of its twisted structure. The significantly larger quadratic polarizability of molecule **3d** than that of **3c** is attributed to the significant lowering of HOMO to LUMO transition energy gap.

4. Conclusion

In the present study, a number of different derivatives of tetradehydrodinaphtho [10] annulene have been considered for the theoretical study of the electronic structure and first hyperpolarizability by employing BHHLYP, CAM-B3LYP and M06-2X functionals. The CAM-B3LYP and M06-2X calculated results, in general, are found to agree within a close margin. Our theoretical study demonstrates that the partial modification of acetylene linkages between two naphthalene rings may lead to significant modulation of longitudinal charge transfer and polarity at the ground state which in turn predicts a dramatic variation of first hyperpolarizability. The electronic nature and planarity of the bridging moiety play a crucial role in the modulation of opto electronic property of the investigated molecules. The heterocyclic ring moieties at the bridge position in conjunction with the acceptor susbstituted thiophene ring fused with the naphthalene ring at the acceptor side are found to predict significantly large first hyperpolarizability. The variation of first hyperpolarizability has been explained satisfactorily in the light of two state model.

5. Acknowledgements

(RSR) acknowledges the UGC BSR (**F.7-223/2009(BSR**) for financial support and (PKN) acknowledges the grant from UGC, Government of India under the Major Research Project (F. No. **42-339/2013 (SR)** for carrying out this research work.

6. References

1. J. M. Squirrell, D. L.Wokosin, J. G.White and B. D. Bavister, *Nat. Biotechnol ,* 1999**,** **17**, 763–767.

2. Y. H. Jiang, Y. C. Wang, J. B. Yang, J. L. Hua, B. Wang, S. Q. Qian and H. Tian, *J. Polym. Sci., Part A: Polym. Chem.*, 2011, **49**, 1830.

3. D. R. Kanis, M. N. Ratner and T. Marks, *J. Chem. Rev*., 1994, **94** , 195.

4. Di Bella, *Chem. Soc. Rev.,* 2001, **30,** 355−366.

5. (*a*) D. S. Chemla and J. Zyss. *Nonlinear Optical Properties of Organic Molecules and Crystals;* Academic Press: New York, 1987; Vol. 1. (*b*) C. W. Spangler*, J. Mat. Chem*., 1999, **9**, 2013–2020. (*c*) Y. Gao, S.L.Sun. H.L. Xu, L. Zhao and Z.M. Su., *RSC Adv.*, 2014, **4**, 24433–24438.

6. D. J. Williams. *Nonlinear Optical Properties of Organic and Polymer Materials;* American Chemical Society: Washington, DC, 1985; *ACS Symposium Serie*s 233.

7. P. R. Prasad and D. J. Williams. *Introduction to Non-linear Optical Effects in Molecules and Polymers*; Wiley: New York, 1991.

8. R.A. Hann and D. Bloor. *Organic Materials for Nonlinear Optics*; Royal Society of Chemistry: London, 1989.

9. L. R. Dalton, A. W. Harper, R. Ghosn, W. H. Steier, M. Ziari, H. Fetterman, Y.Shi, R. V. Mustacich, A. K. Y. Jen and K. J. Shea, *Chem. Mater.,* 1995, **7**, 1060.

10. (*a*) L. T. Chen, W. Tam, S. R. Marder, A. E. Stiegman, G. Rikken and C. W. Spangler, *J. Phys. Chem.,* 1991, **95**, 10643. (*b*) S. R. Marder, D. N. Beratan and L.-T. Cheng, *Science,* 1991, **252**, 103-106.

11. C. M. Whitaker, E. V. Patterson, K. L. Kott and R J. McMahon, *J. Am. Chem. Soc.,* 1996**,** **118***,* 9966-9973.

12. P. K. Nandi, N. Panja and T. K. Ghanty, *J. Phys. Chem. A*, 2008, **112,** 4844−4852.

13. P. K. Nandi, N. Panja and T. K. Ghanty, *J. Phys. Chem. A,* 2009, **113**, 2623−2631.

14. P. K. Nandi, N. Panja and T. K. Ghanty, *Theor. Chem. Acc.*, 2010, **126**, 323−337.

15. K. Hatua and P. K. Nandi, *J. Theor. Comput. Chem*., 2013, **12**, 1250099.

16. (*a*) F. Liu, Y. Yang, S. Cong, H. Wang ,M. Zhang, S. Bo, J. Liu, Z. Zhen, X. Liu and L. Qiu, *RSC Adv*., 2014, **4**, 52991–52999. (*b*) S. R. Marder, C. B. Gorman, F. Meyers, J. W. Perry, G. Bourhill, J. L. Bredas and B. M. Pierce, *Science ,* 1994, **265**, 632−635.

17. F. Meyers, S. R. Marder, B. M. Pierce and J. L. Bredas, *J.Am. Chem. Soc*., 1994, **116**, 10703−10714.

18. X. Zhang, H.Q. Wu, H.L. Xu , S.L. Sun and Z.M.Su, *J. Phys. Chem. A,* 2015, **119**, 767−773.

19. A. S. Ichimura, J. L. Dye, M. A. Camblor and L. A. Villaescusa, *J. Am. Chem. Soc*., 2002, **124**, 1170−1171.

20. W. Chen, Z. R. Li, D. Wu, Y. Li, C. C. Sun and F. L. Gu , *J. Am. Chem. Soc*., 2005, **127**, 10977−10981.

21. S. Muhammad, H. L. Cut, Y. Liao, Y. H. Kan and Z. M. Su, *J. Am. Chem. Soc*., 2009, **131**, 11833−11840.

22. (*a*) H. Xu, D. Yang, F. Liu, M. Fu, S. Bo , X. Liu and Y. Cao, *Phys. Chem. Chem. Phys.,* 2015*,* **17***,* 29679--29688. (*b*) I. D. L. Albert, T. J. Marks and M. A. Ratner, *J. Am. Chem. Soc.,* 1997, **119**, 3155–3156. (*c*) I. D. L .Albert, T. J. Marks and M. A. Ratner, *Chem. Mater*., 1998, **10**, 753–762. (*d*) P. R.Varanasi, A. K. Y. Jen, J. Chandrasekhar, I. N. N. Namboothiri and A. Rathna, *J. Am. Chem. Soc*., 1996, **118**, 12443–12448.

23. Y. Shi, D. Frattarelli, N. Watanabe, A. Facchetti, E. Cariati, S. Righetto, E. Tordin, C. Zuccaccia, A. Macchioni, S. L. Wegener, C. L. Stern, M. A. Ratner and T. J. Marks, *J. Am. Chem. Soc.,* 2015, **137**, 12521−12538.

24. (*a*) G. R. Desiraju and A. Gavezzotti, *J. Chem. Soc., Chem. Commun.,*1989, 621–623. (*b*) A.Gavezzotti and G. R. Desiraju, *Acta Crystallogr., Sect. B* 1988, **44**, 427–434.

25. R. Umeda, D. Hibi, K. Miki, Y. Tobe**,** *Org. Lett.,* 2009,**11**, 4104.

26. M. J. Frisch, G. W. Trucks, H. B. Schlegel, G. E. Scuseria, M. A. Robb, J. R.Cheeseman, G. Scalmani, V. Barone, B. Mennucci and G. A. Petersson et al *Gaussian 09, Revision A.02* Gaussian, Inc., Wallingford CT, 2009.

27. A.D. Becke, *J. Chem. Phys.,* 1993, **98**, 1372-1377.

28. T. Yanai, D. Tew and N. Handy, *Chem. Phys. Lett.,* 2004, **393**, 51 - 57.

29. G.E. Hohenstein, T. S. Chill. D.C. Sherrill, *J. Chem. Theory Comput.,* 2008, **4**, 1996–2000.

30. P.A. Limacher, K.V. Mikkelsen and H.P. Lüthi, *J. Chem. Phys.,* 2009, **130**, 194114-(1-7).

31. A. Alparone, *Chem. Phys. Lett.,* 2011, **514**, 21 - 25.

32. K. Hatua, P.K. Nandi, *J. Phys. Chem. A.,* 2013, **117**, 12581-12589.

33. K. Hatua and P.K. Nandi, *J. Mol. Model.,* 2014, **20**, 2440.

34. J.L. Oudar, *J. Chem. Phys*., 1977, **67**, 446.

35. J.L. Oudar and D.S. Chemla, *J. Chem. Phys*., 1977,**66**,2664.

36. R. Sen, D. Majumdar,; S.P. Bhattacharyya and S.N. Bhattacharyya, *J. Phys. Chem*., 1993**,** **97**, 7491.

37. M. Barzoukas, C. Runser, A. Fort and B.M. Desce, *Chem. Phys. Lett*., 1996, **257** ,531

38. M.J. G. Peach, T. Helgaker, Salek, T.W. Keal, O.B. Lutnæs, D.J. Tozer and N.C. Handy, *Phys. Chem. Chem. Phys.,* 2006, **8**, 558 – 562.

39. B.M. Wong and T.H. Hsieh, Theory. *J. Chem. Theory Comput.,* 2010**, 6***,* 3704–3712.

40. W. Zhu and Y. Jiang, *Phys. Chem. Chem. Phys*., 1999, **1**, 4169-4173.

Table1 Important bond angles and torsion angles (in degree) of molecules of **scheme I-III**

Schemes I and **II**

Molecules	Angle $<C_1C_{20}C_{19}$	Molecules	Angle $<C_{10}C_{11}C_{12}$
1a	175.1	**1c**	172.3
1b	174.8	**2b**	160.3
2a	161.4		
	$<C_{11}C_{12}C_{13}$		$<C_{14}C_{15}C_{16}$
2c	148.4	**2d**	148.6

Scheme III

Molecules	$\tau_{C9C10C1C20}$	Molecules	$\tau_{C22C21C10C11}$
3a	27.9	**3b**	24.5
3c	1.4	**3c**	1.3

Table 2 Ground state dipole moment (μ, debye) and first hyperpolarizability (**β**, au) of molecules of **scheme I** obtained at different DFT functionals for the 6-311++G(d,p) basis set

		1a	**1b**	**1c**
BHHLYP	μ_x	0.000	14.929	14.369
	μ_g	0.000	15.199	14.698
	β_x	0.3	79424.6	125882.0
	β_0	0.4	80047.0	127164.0
CAM-B3LYP	μ_x	0.000	14.517	13.854
	μ_g	0.000	14.771	14.187
	β_x	0.3	79727.5	138453.0
	β_0	0.4	80304.0	139658.0
M06-2X	μ_x	0.000	14.675	13.972
	μ_g	0.000	14.929	14.340
	β_x	0.323	80458.4	135520.0
	β_0	0.3	81013.0	136657.5

Table 3 Ground state dipole moment (μ, debye) and first hyperpolarizability (**β**, au) of molecules of **scheme II** obtained at different DFT functionals for the 6-311++G(d,p) basis set

		2a	**2b**	**2c**	**2d**
BHHLYP	μ_x	19.735	23.975	12.769	-13.761
	μ_g	19.755	23.975	12.923	13.895
	β_x	-50546.4	63896.3	-118584.0	183839.0
	β_0	50654.5	65364.0	118838.0	184087.5
CAM-B3LYP	μ_x	19.158	23.573	12.180	-12.789
	μ_g	19.177	23.586	12.323	12.919
	β_x	-59925.5	68649.1	-108521.0	208766.0
	β_0	60123.5	70135.0	108811.0	208972.0
M06-2X	μ_x	19.240	23.394	12.350	-12.911
	μ_g	19.261	23.415	12.495	13.067
	β_x	-58962.9	60664.7	-110796.0	204638.0
	β_0	59157.0	61910.5	111097.0	204864.0

Table 4 Ground state dipole moment (μ, debye) and first hyperpolarizability (**β**, au) of molecules of **scheme III** obtained at different DFT functionals for the 6-311++G(d,p) basis set

		3a	**3b**	**3c**	**3d**
BHHLYP	μ_x	-18.371	-16.187	13.490	13.205
	μ_g	18.533	16.493	13.793	13.497
	β_x	28422.7	45628.5	-110809.0	-189212.0
	β_0	28640.3	45733.6	111497.0	190597.0
CAM-B3LYP	μ_x	17.902	-15.815	13.089	12.476
	μ_g	18.058	16.117	13.378	12.783
	β_x	29921.5	50885.3	-102668.0	-211412.0
	β_0	30153.8	51052.0	103259.0	212679.0
M06-2X	μ_x	-17.779	-15.744	13.361	12.810
	μ_g	17.942	16.086	13.644	13.144
	β_x	30051.1	53022.6	-105788.0	-197779.0
	β_0	30287.9	53271.5	106385.5	199018.5

Table 5 Transition energy (ΔE_{eg}, au), transition moment (μ_{eg}, D), dipole monent difference ($\Delta\mu_{eg}$, au), oscillator strength (f_{eg}, au) and two state calculated first hyperpolarizability (β_0, au) corresponding to the most intense electronic transition ($S_0 \rightarrow S_n$) obtained at the CAM-B3LYP level for the 6-311++G(d,p) basis set

Molecule	ΔE_{eg}	μ_{eg}	$\Delta\mu_{eg}$	f_{eg}	β_0	Electronic transition	Orbital transition
1a	0.11729	7.923	0.000	0.755	0.18	S0 → S1	HOMO → LUMO
1b	0.08854	9.179	3.586	0.765	3952.33	S0 → S1	HOMO →LUMO
1c	0.06179	9.866	1.662	0.616	4338.64	S0 → S1	HOMO →LUMO
2a	0.07067	9.710	0.785	0.683	1518.75	S0 →S2	HOMO → LUMO
2b	0.05728	8.437	1.268	0.418	2820.43	S0 →S2	HOMO → LUMO
2c	0.07492	6.883	4.309	0.364	3729.26	S0 →S1	HOMO → LUMO
2d	0.04954	8.858	1.806	0.398	5911.65	S0 → S1	HOMO → LUMO
3a	0.10941	6.235	1.044	0.436	347.62	S0 → S7	HOMO → LUMO
3b	0.07340	5.935	1.335	0.265	894.90	S0 → S4	HOMO → LUMO+1
3c	0.08625	7.507	4.679	0.498	3632.08	S0 →S2	HOMO → LUMO
3d	0.05191	8.145	2.129	0.353	5373.14	S0 → S1	HOMO → LUMO

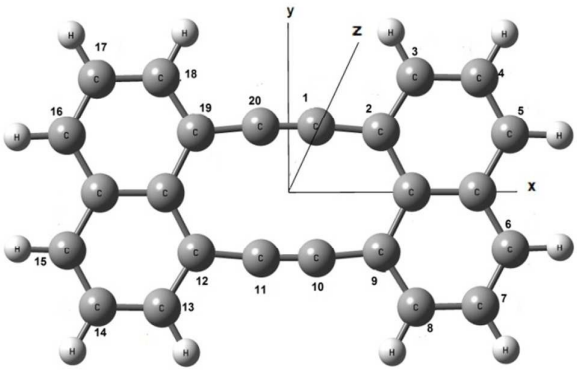

1a

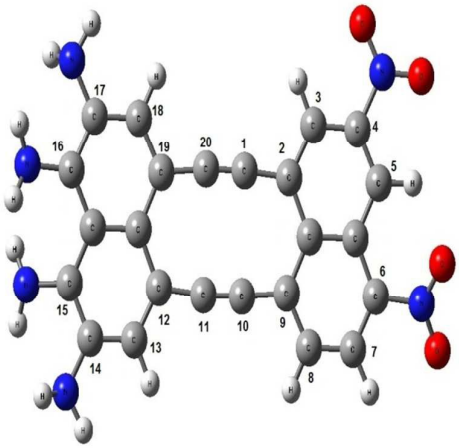

1b

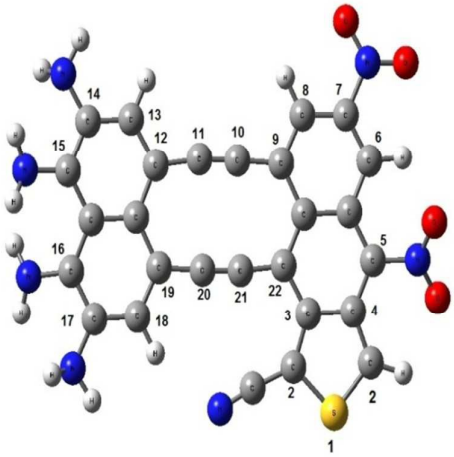

1c

Scheme I: Molecules containing acetylene bridging unit

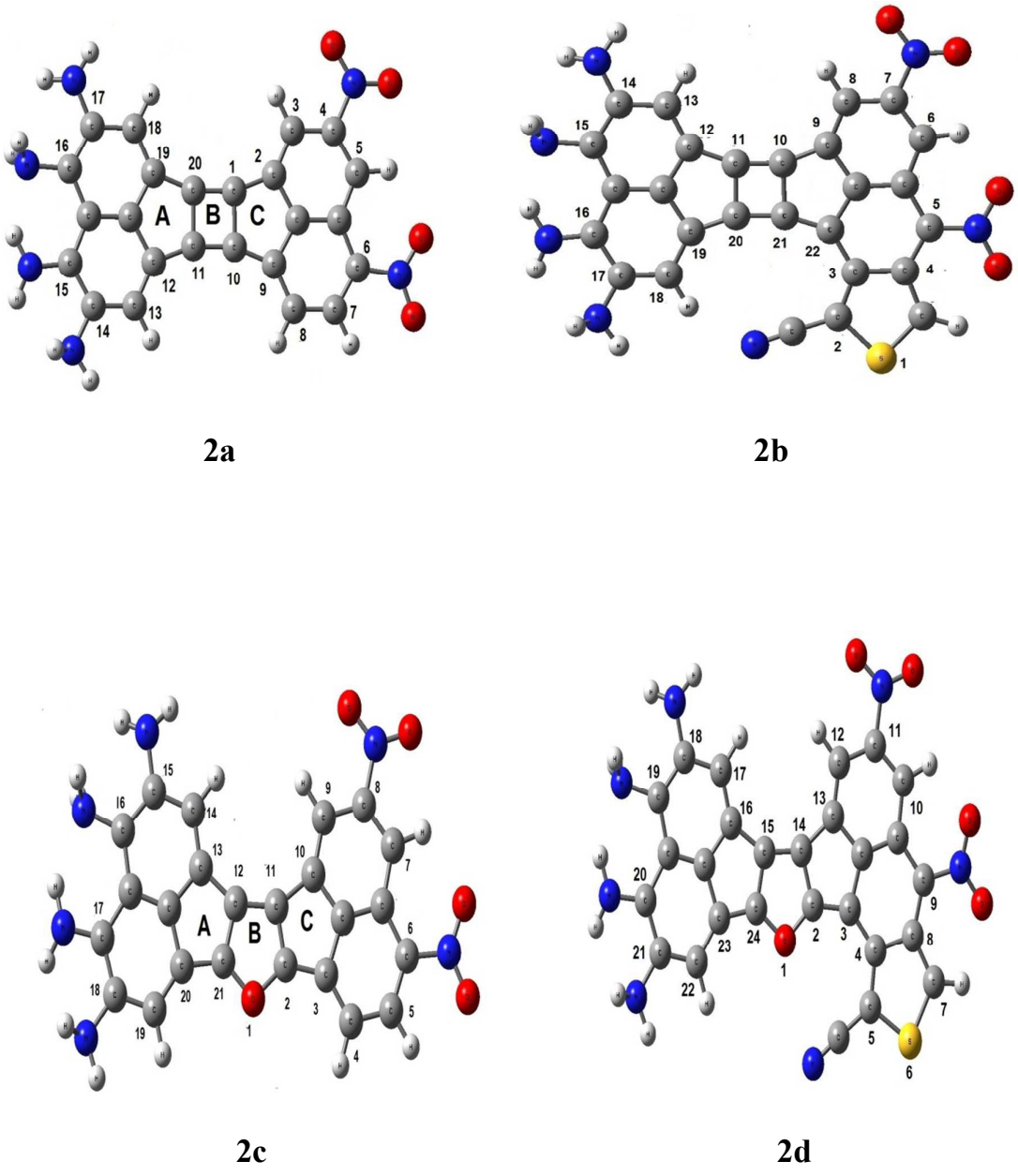

2a **2b**

2c **2d**

Scheme II: Molecules containing cyclobutadiene ring (**2a** and **2b**) and furan ring (**2c** and **2d**) fused with two adjacent cyclo pentadiene rings as bridging units.

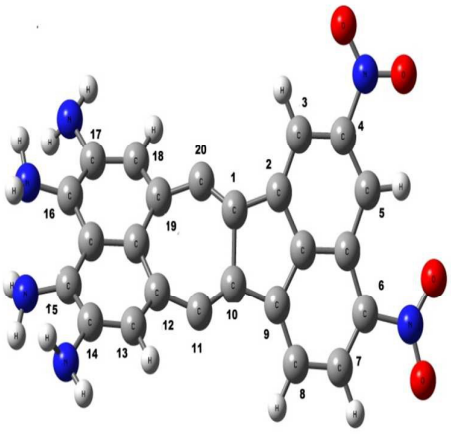

3a

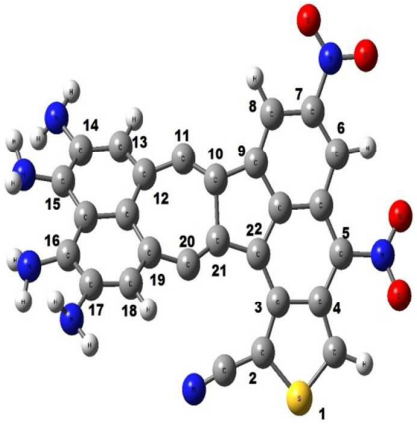

3b

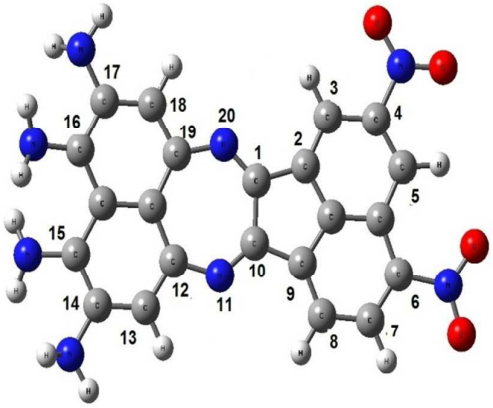

3c

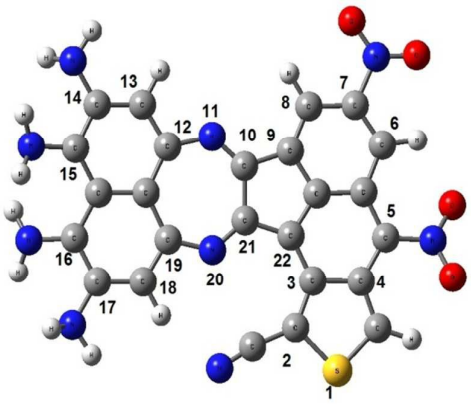

3d

Scheme III: Molecules containing azulene ring (3a and 3b) and heteroazulene ring (3c and 3d) as bridging units.

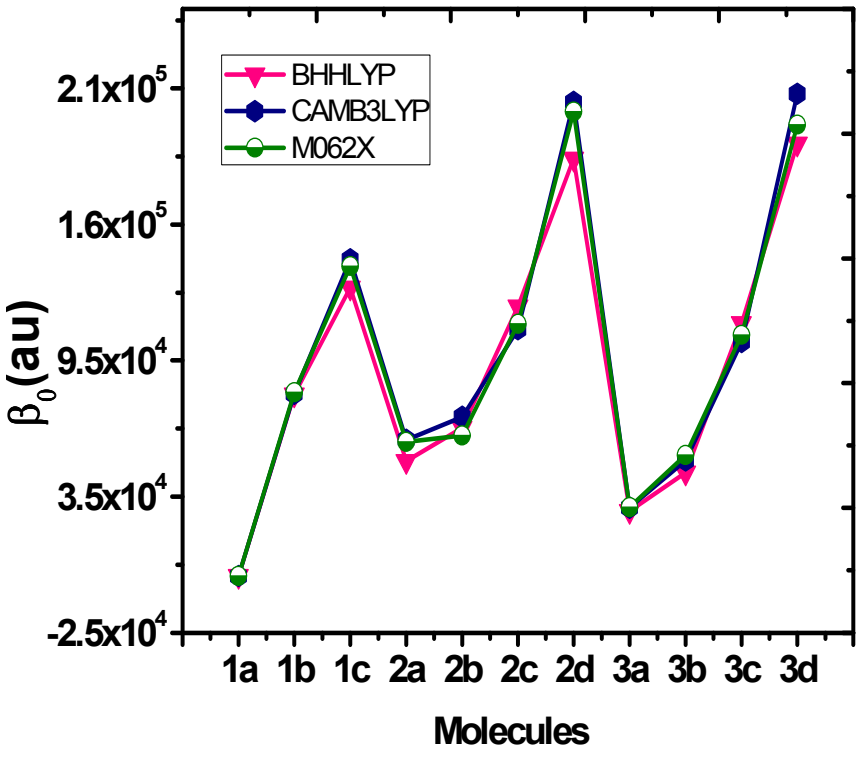

Fig.1 The variation of first hyperpolarizability among molecules of **Schemes I – III**.

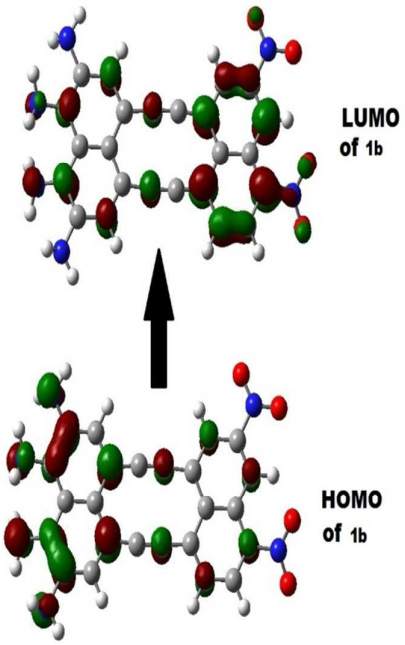

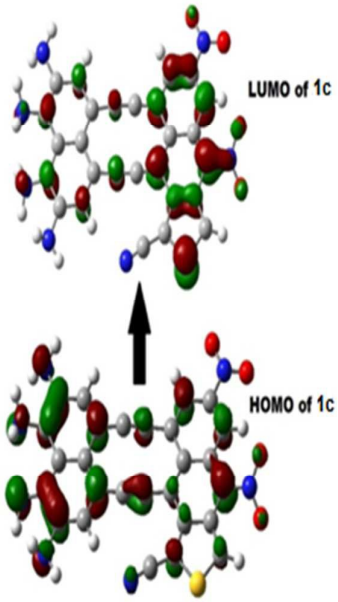

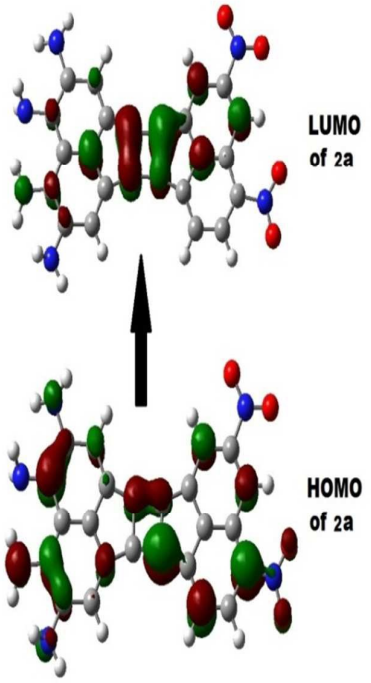

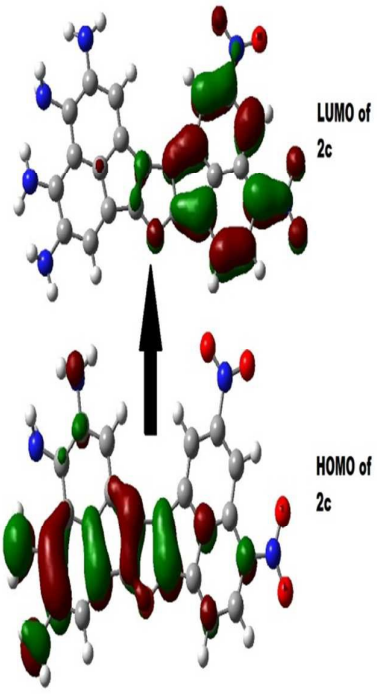

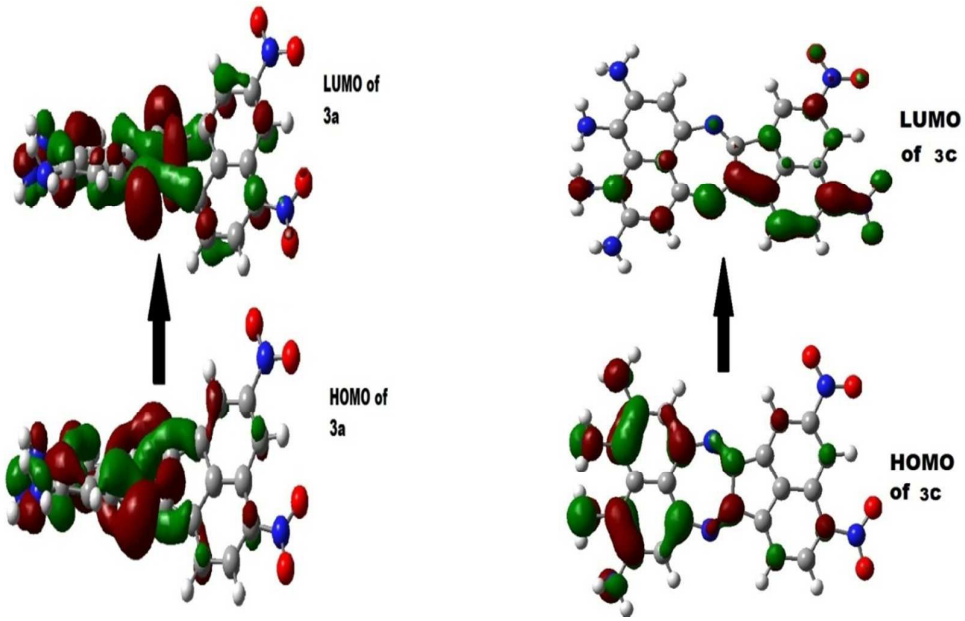

Fig. 2 The frontier orbital pictures of some representative molecules of **Schemes I – III**.

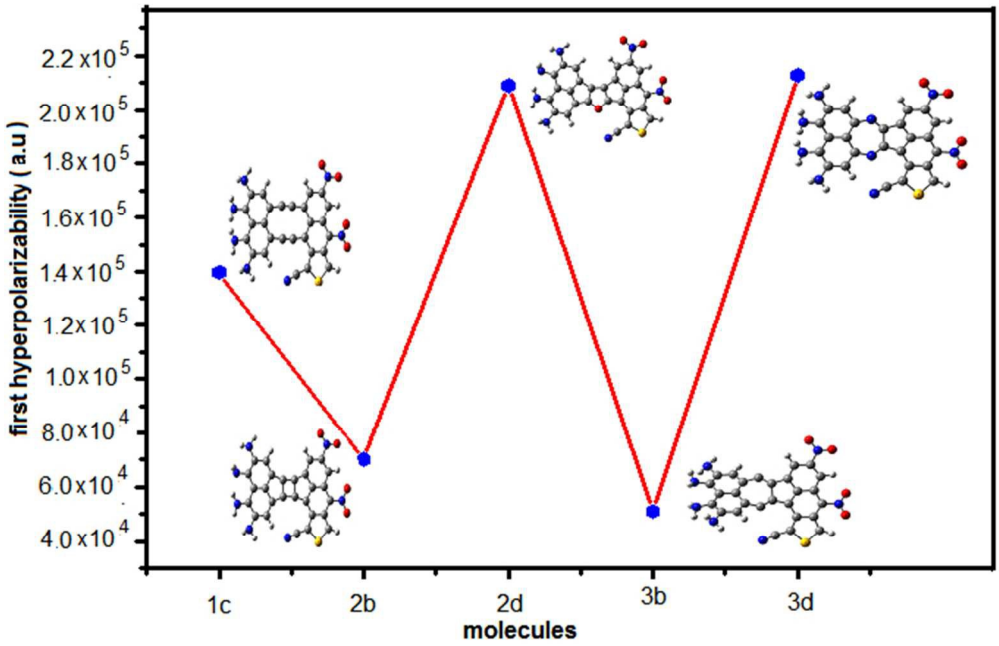

180x116mm (96 x 96 DPI)